

Design and Evaluation of a Workload-Adaptive Haptic Shared Control Framework for Semi-Autonomous Driving

Yifan Weng, Ruikun Luo, Paramsothy Jayakumar, Mark J. Brudnak, Victor Paul, Vishnu R. Desaraju, Jeffrey L. Stein, X. Jessie Yang, Tulga Ersal*

Abstract—Haptic shared control of an autonomy-enabled vehicle is used to manage the control authority allocation between a human and autonomy smoothly. Existing haptic shared control schemes, however, do not take the workload condition of human into account. To fill this research gap, this study develops a novel haptic shared control scheme that adapts to a human operator’s workload in a semi-autonomous driving scenario. Human-in-the-loop experiments with 8 participants are reported to evaluate the new scheme. In the experiment, a human operator and an autonomous navigation module shared the steering control of a simulated teleoperated vehicle in a path tracking task while the speed of the vehicle is controlled by autonomy. High and low screen refresh rates were used to create moderate and high workload cases, respectively. Results indicate that adaptive haptic control leads to less driver control effort without sacrificing the path tracking performance when compared with the non-adaptive case.

I. INTRODUCTION

Haptic shared control of a vehicle is a semi-autonomous driving mode that enables smooth transitions of control authority and allows the human to negotiate with autonomy [1]–[5]. In this driving mode, both the human and autonomy express their intention through the torques they apply on the steering wheel, the angle of which has a one-to-one correspondence to the angle of the tires. This scheme enables negotiation between the two agents; the human can feel the autonomy’s intention through the torque autonomy applies to the steering wheel and fully or partially yield to or override autonomy by reducing or increasing his/her impedance.

In haptic shared control, the impedance of autonomy is also critical for the negotiation and considered as a design parameter. Some research efforts focus on the fixed impedance scheme [1], [4], [5], while others explore modifying the impedance of autonomy based on some design principles [2], [3]. Majority of the latter group considers an adaptive law based on the vehicle-performance-based metrics such as deviation from the path [2]. However, human factors related metrics are also important to consider for successful transitions of control authority. An example such metric considered in the literature is attention on the road [3].

Workload is another important human factor related to human performance [6]. In general, workload of the human

We acknowledge the technical and financial support of the Automotive Research Center (ARC) in accordance with Cooperative Agreement W56HZV-14-2-0001 U.S. Army Ground Vehicle Systems Center (GVSC) Warren, MI.

Y. Weng, J. L. Stein, and T. Ersal are with the Department of Mechanical Engineering, University of Michigan, Ann Arbor, MI.

R. Luo is with the Robotics Institute, University of Michigan, Ann Arbor, MI.

P. Jayakumar, M. J. Brudnak, and V. Paul are with the U.S. Army Ground Vehicles System Center, Warren, MI.

V. R. Desaraju is with Toyota Research Institute, Ann Arbor, MI.

X. J. Yang is with the Department of Industrial and Operations Engineering, University of Michigan, Ann Arbor, MI.

* Corresponding author. Email: tersal@umich.edu

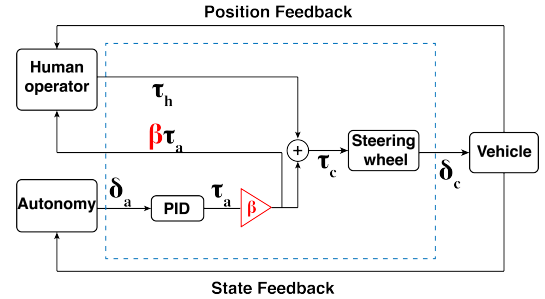


Fig. 1: Block diagram for haptic shared control. δ_a represents the steering angle command from autonomy, τ_h and τ_a represent the torque from human and autonomy, respectively. τ_c and δ_c are the resultant torque and actual control steering angle. β is the assistance level, which is always 1 in the baseline non-adaptive scheme, whereas it varies in the proposed adaptive scheme.

operator varies as the driving conditions change [7]. These variations in workload have a direct impact on the proper management of control authority, as the human operator may or may not perform as expected based on their current workload [8]. However, workload has not yet been considered as a factor in the adaptation of the impedance of autonomy in haptic shared control of vehicles.

In this paper, we aim to address this gap by designing and testing a workload-adaptive framework for haptic shared control of a vehicle. The adaptive scheme considers the workload of the human operator as well as their steering torque, which is interpreted as an expression of intention for intervention. We then examine the performance of the proposed adaptive scheme compared with the traditional non-adaptive one through a human-in-the-loop experiment, in which the human operator’s workload is regulated by controlling the screen refresh rate.

The rest of the paper is organized as follows. Sec. II describes the design of the haptic shared control schemes. Sec. III describes the algorithm for autonomy used in this work. The design of the human-in-the-loop experiment is given in Sec. IV. Sec. V presents the results and discussion. The paper concludes with Sec. VI.

II. HAPTIC SHARED CONTROL FRAMEWORK

The block diagram for haptic shared control used in this work is shown in Fig. 1. This scheme is implemented in a human-in-the-loop simulation setting.

The torque τ_a reflects the autonomy’s intention and is applied through a torque feedback feature on the steering wheel. This torque is generated through a proportional-integral-derivative (PID) controller that tracks the reference steering angle generated by the autonomy module using the nonlinear model predictive control (NMPC) formulation described in Sec. III. This formulation aims to track a given

path, and generates also the speed commands in addition to the reference steering angle. The PID is tuned such that the vehicle can track the perceived path even without any human intervention. It is, however, unable to perceive and avoid any obstacles on the path.

The real path is denoted with white dashed lines on the road called the centerline. Perceived path from the autonomy's point of view may be different from the real one when perception challenges exist. The simulation testbed has the capability to emulate such a scenario by introducing a bias between the perceived and real path.

Through this haptic shared control design, the human operator can feel the torque from autonomy and negotiate with it, leading to a smooth control authority transfer. The human torque is denoted with τ_h .

The resultant torque τ_c combining both the one from autonomy τ_a and the one from human operator τ_h determines the final control input to the vehicle, namely, the steering angle δ_c .

Two haptic shared control schemes are considered: the proposed adaptive one, and a non-adaptive one as the baseline. They are described further in detail next.

A. Adaptive haptic shared control

The adaptive scheme is designed based on two variables: workload of and input torque from the human operator. Workload reflects the condition of the human operator, whereas the input torque indicates human's level of disagreement with autonomy. The resultant torque in Fig. 1 is calculated in this scheme as

$$\tau_c = \tau_h + \beta(w_t, \hat{\tau}_h)\tau_a, \quad (1)$$

where the term β is referred to as the assistance level. It represents the magnitude of assistance from autonomy, thus controlling its impedance. $\hat{\tau}_h$ is the human's normalized input torque, which is calculated by dividing the human's torque τ_h by an estimate of the maximum value $\tau_{h,\max}$ the human operator can apply. In the developed testbed, $\tau_{h,\max}$ is set as 1.7 Nm based on pilot human-subject studies. By modifying the assistance level β , the impedance can be varied in a manner adaptive to the workload of and torque exerted by the human operator in contrast to a fixed impedance in the non-adaptive scheme, where β is always 1.

The assistance level β is heuristically designed based on two aspects. The first aspect considers the human's performance under different workload conditions. As shown in Fig. 2a, for a given amount of torque exerted by the human operator, level of assistance from autonomy varies with the workload of the human. The curve is designed according to the principle described in [9]. It indicates that human operator should receive less support in the moderate workload region than in the overloaded or underloaded regions, because a moderate workload is considered optimal for human performance. In the present study, w_t is defined such that $w_t = 0$ represents the underloaded cases, $w_t = 50$ the moderate workload cases, and $w_t = 100$ the overloaded cases. When human operator has moderate workload ($w_t = 50$), β is set to be the lowest value among the whole workload spectrum. In particular, a value is chosen that is close to zero, but not too small to the extent that the human does not feel autonomy's torque and hence intent anymore. Specifically, $\beta = 0.1$ for moderate workload when human operator

exerts the maximum torque. When the human operator is underloaded ($w_t = 0$) or overloaded ($w_t = 100$), $\beta = 1$ to provide full support from autonomy. Sigmoid functions are used to connect the moderate workload case and the underloaded and overloaded cases smoothly.

As for the second design aspect, for a given workload the human operator experiences, larger torque input from the human indicates a stronger disagreement with autonomy. Emergency cases may require such strong interventions. Hence, the assistance level is reduced with a goal to make it easier for the human to control the vehicle as he/she applies more torque as shown in Fig 2b. However, the level of reduction in the assistance level depends on the human's workload. Since a moderate workload level is considered optimal in the literature [9], when the human operator has moderate workload, his/her command is considered to be more reliable compared with the overloaded or underloaded cases. Therefore, the assistance level β is reduced more when $w_t = 50$ than the cases when $w_t = 0$ or $w_t = 100$. For all these cases, β starts from 1 to navigate the vehicle in autonomous mode when the human operator has no input torque. This assistance level is maintained until reaching a threshold to filter out small unintended torques. In the cases when human operator experiences moderate workload and completely yields to autonomy, this threshold is set to around 0.04 Nm and the corresponding normalized torque is calculated to be 0.02. This threshold is determined based on pilot human-subject studies. Similarly, the threshold for under and overloaded cases ($w_t = 0$ or $w_t = 100$) is picked as 0.3. A quadratic function, which is symmetric about $w_t = 50$, is used to connect these values in three different cases to model the threshold for different workload values w_t . Thus, for a given workload, the threshold and assistance level are calculated when human exerts the maximum torque ($\hat{\tau}_h = 1$). The smooth transitions along the dimension of normalized human torque is achieved through a sigmoid function.

Combining these two aspects, the assistance level β is calculated as

$$\beta(w_t, \hat{\tau}_h) = 1 - \left[1 - \left(\frac{0.9e^{0.3(|w_t-50|-25)}}{e^{0.3(|w_t-50|-25)} + 1} + 0.1 \right) \right] \cdot \left[\frac{e^{\frac{60\hat{\tau}_h - 18.6 - 8.4(\frac{w_t}{50} - 1)^2}{2.9 - 1.4(\frac{w_t}{50} - 1)^2}}}{e^{\frac{60\hat{\tau}_h - 18.6 - 8.4(\frac{w_t}{50} - 1)^2}{2.9 - 1.4(\frac{w_t}{50} - 1)^2}} + 1} \right]. \quad (2)$$

and the corresponding 3D plot showing the relationship between the assistance level β , the workload w_t and the normalized human torque $\hat{\tau}_h$ is shown in Fig. 3.

B. Baseline non-adaptive haptic shared control

For the baseline non-adaptive scheme, the torque from the autonomy is directly blended with the torque from the human operator. In the control diagram shown in Fig. 1, $\beta = 1$ for all times in this scheme.

III. DESIGN OF AUTONOMY IN SHARED CONTROL

A nonlinear model predictive control (NMPC) based navigation algorithm is used as the autonomy in this study. It provides references for the steering angle and speed commands. The NMPC formulation is adopted from [10] and [11] with modifications. In particular, a new cost function is designed

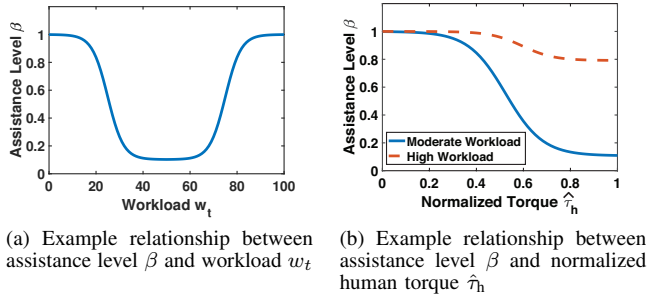


Fig. 2: Illustration of design principles of assistance level

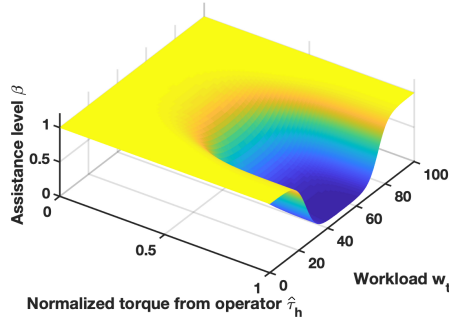


Fig. 3: Relationship between base assistance level β , workload w_t , and normalized human input torque $\hat{\tau}_h$

to fit the context of this work, while the vehicle models and most of the constraints for states and controls are the same as in the literature [10], [11], the only difference being that obstacle avoidance constraints are not employed in this work. Hence, autonomy is only capable of tracking a given path. The cost function is modified, because the path tracking task in this work differs from the task of navigating unstructured environments considered in [10], [11]. Specifically, the cost function in this study is

$$\begin{aligned}
 J = & w_1 T_p + w_2 \int_{t_0}^{t_P} \left(y_{\text{ref}}(x(t)) - y(t) \right)^2 dt \\
 & + w_3 \int_{t_0}^{t_P} (w_\gamma \gamma^2 + w_{J_x} J_x^2) dt \\
 & + w_4 \int_{t_0}^{t_P} \tanh \left[-\frac{F_{z,rl} - a}{b} \right] + \tanh \left[-\frac{F_{z,rr} - a}{b} \right] dt.
 \end{aligned} \quad (3)$$

It consists of four terms. The first term is used to control the speed of the vehicle. T_p is the prediction horizon calculated by traveling a constant distance, which is 100 m in this study. The second term penalizes the deviation from the current position of the vehicle $y(t)$ to the given position on the path $y_{\text{ref}}(x(t))$. The third term regulates the control inputs of the vehicle, namely, the longitudinal jerk J_x and steering rate γ , for a smooth steering maneuver and acceleration. Two weights w_{J_x} and w_γ are set to balance the regularization of these two control inputs. The fourth term is a soft constraint that increases the cost when one of the tire vertical loads $F_{z,rl}$, $F_{z,rr}$ is close to the lowest allowable threshold. This soft constraint is used to prevent the vehicle from operating at its dynamic limit unnecessarily [10], [12]. Four weights

w_1 , w_2 , w_3 and w_4 are set to achieve a trade-off between these goals. The cost function integrates the terms starting from t_0 , the moment when autonomy receives a new piece of information about vehicle, to t_p , the moment the prediction ends. t_p is calculated as $t_0 + T_p$.

A constant bias of 0.8 m is added to the real trajectory in the cases where a perception challenge was emulated. The bias is selected to be large enough to differ from the unbiased case clearly, but not too large to render autonomy useless.

To solve the NMPC problem, the open-source nonlinear optimal control package NLOptControl [13] is used, which adopts the Legendre-Gauss-Radau collocation method to transfer the continuous optimal control problem into a nonlinear program. The nonlinear program is then solved by using the solver package IPOPT [14]. This optimization process generates a series of steering angle and speed commands through the whole control horizon T_p , and only the first 3 s worth of commands is buffered for use. While executing the previous control command series, the system formulates and solves a new optimal control problem with a receded horizon, and the resulting new command series are applied as soon as they are available. Hence, the control update time is variable. In the current study, the maximum update time during the experiment driving was 0.57 s, while the median update time was 0.22 s. These update times are sufficient in light of prior work [10]–[12].

IV. EXPERIMENT DESIGN

A. Experimental Setup

We used a human in the loop experiment to evaluate the performance of the adaptive control scheme. We developed our testbed based on the teleoperated vehicle simulation setup of [15] as shown in Fig. 4. More specifically, the human operator and the autonomy shared the steering control of a simulated teleoperated vehicle, namely, a notional High Mobility Multipurpose Wheeled Vehicle (HMMWV). At the same time, autonomy controlled the speed of the vehicle. The autonomy in this experiment was based on the NMPC approach as described in Sec. III. To regulate the workload, the human participant was exposed to different screen refresh rates. We hypothesized that in a high refresh rate case (20 Hz, or a refresh period of 0.05 s per frame), the human operator experiences a moderate workload level, while in a low refresh rate case (2.5 Hz, or refresh period of 0.4 s per frame), the human participant needs to use more mental resource to interpolate the vehicle's behavior between two frames and thus experiences an overloaded case. The validity of this hypothesis was tested as part of the experiment. The autonomy would also exhibit different performance levels introduced through a bias in the perceived path to emulate a perception challenge for the autonomy.

We investigated the performance for two different haptic shared control schemes in the human-in-the-loop experiment: the adaptive haptic shared control and non-adaptive haptic shared control schemes. The adaptive haptic shared control scheme adapted to the perceived workload corresponding to the screen refresh rate the human operator experienced and the torque input from human operator.

B. Methodology

1) *Participants*: A total of 8 students participated in the experiment. These 8 participants were on average 22.9 years



Fig. 4: Shared control simulation platform

TABLE I: Eight Test Conditions

Condition	Autonomy Performance	Screen Refresh Rate	Haptic Shared Control Scheme
1	Unbiased	20 Hz	Non-adaptive
2	Unbiased	20 Hz	Adaptive
3	Biased	20 Hz	Non-adaptive
4	Biased	20 Hz	Adaptive
5	Unbiased	2.5 Hz	Non-adaptive
6	Unbiased	2.5 Hz	Adaptive
7	Biased	2.5 Hz	Non-adaptive
8	Biased	2.5 Hz	Adaptive

old ($SD = 3.6$ years) and had an average of 4.1 years of driving experience ($SD = 3.5$ years). All participants had normal or corrected-to-normal vision.

2) *Driving Task*: In the driving task, a participant and the autonomy shared the steering control of the vehicle, whereas the speed of the vehicle was controlled by autonomy. The goal of the task is to complete a track with minimal deviation from the path as denoted by the centerline without hitting an obstacle. The autonomy had no obstacle avoidance capability. In some cases, to emulate a perception challenge, an offset was introduced such that the autonomy tracked a path that deviated from the centerline by 0.8 m, which is referred to as biased autonomy. To regulate the workload of the subject, 2 screen refresh rates, 20 Hz and 2.5 Hz, were presented. We consider cases where the screen refresh rate is 20 Hz as moderate workload and the cases with the screen refresh rate of 2.5 Hz as high workload. Both non-adaptive shared control scheme and adaptive shared control scheme were used in this experiment as described in Sec. II-B and Sec. II-A, respectively.

3) *Experimental Design*: The experiment used a within-subjects design with three independent variables. The first independent variable was the haptic shared control scheme (adaptive haptic shared control vs. non-adaptive haptic shared control). The second independent variable was the screen refresh rate (20 Hz vs. 2.5 Hz). The third independent variable was the performance of the autonomy (biased vs non-biased). Each participant experienced 8 tracks in the experiment. On each track, one combination of haptic shared control scheme, screen refresh rate and performance of autonomy was used. The resulting eight test conditions are shown in Table I. The presentation of test conditions followed a 8×8 Latin square design to eliminate potential order effects.

4) *Measures*: Five dependent variables were collected in the experiment: participants' self-reported workload and trust in the shared control autonomy, participants' control effort and driving task performance for path tracking period of the driving and participant's control effort during the obstacle avoidance maneuver. After each track, participants reported

their workload and trust using two uni-dimensional scales (see Appendix I). The NASA TLX survey [16] and the Moray's trust survey [17] were presented to the participants before the evaluation stage such that they understood the meaning of workload and trust.

Participants' control effort was calculated as the average torque that a participant applied on the steering wheel. The measurement was acquired at the frequency of 100 Hz by a torque sensor. Driving task performance was evaluated by the path tracking error. The path tracking error is calculated as the mean of the absolute deviation of the vehicle's position from the centerline. The measurement was acquired at the frequency of 100 Hz.

5) *Experimental Procedure*: Participants provided a signed informed consent form and filled in a demographic survey. During the training session, the participants performed five trials of the driving task in different conditions: one with 20 Hz refresh rate, non-adaptive scheme with an unbiased autonomy and four trials with 2.5 Hz refresh rate. They experienced non-adaptive with an unbiased autonomy, adaptive with a biased autonomy, adaptive with an unbiased autonomy and non-adaptive with a biased autonomy. Each trial took approximately 2.5 min.

During the real experiment, participants performed the driving task on 8 different tracks with different test cases as described in Table I. Each trial took approximately 1.5 min. After each trial, the participants were asked to fill a post survey about the workload and trust during the track they just drove on. If they hit the obstacle, the trial was restarted.

V. EXPERIMENTAL RESULTS AND DISCUSSION

Three-way repeated measures Analysis of Variance (ANOVA) was conducted with the shared control scheme, autonomy performance and screen refresh rate as the within-subjects variables. Results are reported as significant for a statistical significance level of $\alpha = 0.05$; i.e., if the probability p of observing the difference seen in the experimental data purely due to random effects is less than 5%, the difference is deemed statistically significant. Table II summarizes the mean and standard error (SE) values of the participants' self-reported workload, self-reported trust, driving task performance and their exerted torque during the path tracking stage and the torque during obstacle avoidance.

1) *Participants' Workload*: Both screen refresh rate and autonomy performance had an impact on the participant's self-reported workload as shown in Fig. 5. The effect of different schemes was not significant. With the 20 Hz screen refresh rate, participants reported lower workload ($F(1, 61) = 20.02$, $p < 0.001$). One reason could be that in the cases when the screen refresh rate was 2.5 Hz, the human operator needed to use more mental resources to interpolate between two frames. This result validated the design of regulating workload in this experiment.

When there was no bias for autonomy, participants reported lower workload ($F(1, 61) = 18.03$, $p < 0.001$). This may result from the fact that the human operator may exert more steering effort for fighting with autonomy in biased case compared with non-biased cases. Nevertheless, in the experimental design, only refresh rate is designed to affect the workload. The workload increase due to bias was not considered and thus results may improve if the workload due to bias is also taken into account in the adaptive scheme.

TABLE II: Mean and Standard Error (SE) of workload, trust, lane keeping error, torque during centerline tracking and torque during obstacle avoidance

Metrics	N	Screen Refresh Rate							
		20 Hz				2.5 Hz			
		Unbiased Autonomy		Biased Autonomy		Unbiased Autonomy		Biased Autonomy	
	Adaptive	Non-adaptive	Adaptive	Non-adaptive	Adaptive	Non-adaptive	Adaptive	Non-adaptive	
Workload	8	4.00 ± 0.94	2.88 ± 0.52	7.63 ± 2.15	9.25 ± 1.39	8.25 ± 1.71	9.13 ± 2.06	11.00 ± 1.50	15.00 ± 1.57
Trust	8	5.88 ± 0.52	6.25 ± 0.25	4.13 ± 0.67	4.00 ± 0.53	5.25 ± 0.56	4.75 ± 0.53	3.63 ± 0.42	3.00 ± 0.46
Centerline tracking error (m)	8	0.19 ± 0.019	0.18 ± 0.022	0.27 ± 0.036	0.32 ± 0.036	0.26 ± 0.039	0.28 ± 0.026	0.48 ± 0.029	0.52 ± 0.047
Torque for centerline tracking stage (Nm)	8	0.19 ± 0.012	0.18 ± 0.011	0.45 ± 0.033	0.99 ± 0.044	0.17 ± 0.024	0.23 ± 0.017	0.44 ± 0.076	0.79 ± 0.084
Torque for obstacle avoidance (Nm)	8	0.35 ± 0.020	0.53 ± 0.036	0.43 ± 0.035	0.76 ± 0.070	0.54 ± 0.049	0.57 ± 0.043	0.73 ± 0.052	1.01 ± 0.095

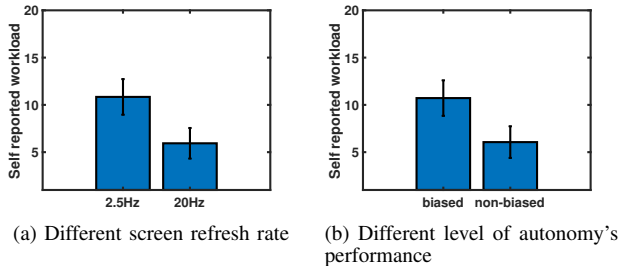


Fig. 5: Mean and standard error (SE) values of self-reported workload with different conditions

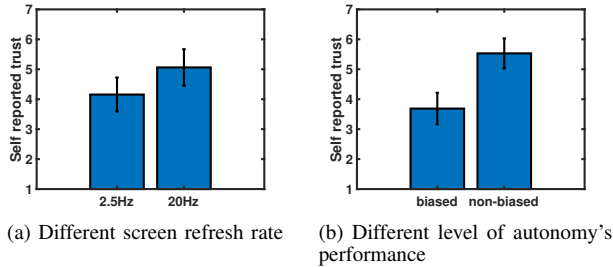


Fig. 6: Mean and standard error (SE) values of self-reported trust with different conditions

2) *Trust in Automation*: Both screen refresh rate and performance of autonomy have an impact on the participant's self-reported trust as shown in Fig. 6. The effect of schemes on trust was not significant.

On the one hand, participants trusted the shared control autonomy more when the autonomy was non-biased ($F(1, 61) = 27.13, p < 0.001$). Since the performance degraded when the autonomy had bias, the result supports prior research that the human operator's trust in automation depends on the autonomy's performance [18], [19].

On the other hand, they also trusted the autonomy more when the screen refresh rate is 20 Hz ($F(1, 61) = 6.56, p = 0.013$). This may result from the fact that information on the environment was abundant in the cases when screen refresh rate was 20 Hz. Human participants could evaluate the performance of the autonomy better, generating more trust towards the autonomy.

3) *Driving Task Performance*: Results revealed that there was no significance in the path tracking error between two shared control schemes as shown in Fig. 7. On the other hand, the performance was significantly worse when low refresh rate was presented compared with the high refresh rate case ($F(1, 61) = 38.47, p < 0.001$). Moreover, the performance was also worse when a biased autonomy was implemented ($F(1, 61) = 54.12, p < 0.001$). These results also reveal that the refresh rate as well as bias have a impact

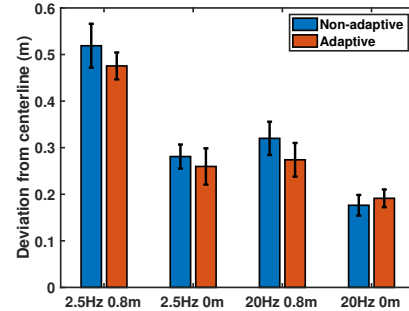


Fig. 7: Lateral control performance in path tracking stage of the driving task for the four conditions of 20 Hz vs. 2.5 Hz refresh rate and 0 m vs. 0.8 m bias in the perception of the path.

on the performance, alongside with the workload reported by human participants.

4) *Participants' Control Effort in Path Tracking*: Results revealed that the adaptive scheme reduces the torque applied by the human operator compared with non-adaptive case ($F(1, 61) = 47.53, p < 0.001$). Specifically, when the autonomy had bias, the human exerted significantly less torque compared with non-adaptive scheme as shown in Fig. 8. On the one hand, when the autonomy had a relatively better performance, the human operator had a higher trust towards the autonomy, leading to the fact that human operator yielded to autonomy more. Therefore, there is almost no difference between two schemes, since in the adaptive scheme, we set the assistance level to be 1 when the torque is small, i.e., when human yields to autonomy. On the other hand, when the autonomy had some bias and human operator needed to intervene to achieve the task objective, the control effort is less when the adaptive scheme was utilized. This observation shows that the adaptive scheme could reduce the control effort, helping the human operator correct the biased guidance from the autonomy easier. Moreover, the human participant also needs to apply significantly higher torque in biased case than the non-biased case. ($F(1, 61) = 202.98, p < 0.001$) while the impact from the refresh rate is not significant.

5) *Participants' Control Effort in Obstacle Avoidance*: Results revealed that the adaptive scheme reduces the torque applied by the human operator compared with non-adaptive case ($F(1, 61) = 29.08, p < 0.001$). Specifically, when the autonomy had bias, the human exerted significantly less torque compared with non-adaptive scheme as shown in Fig. 9. The control effort was less when adaptive scheme was implemented. Just as the previous section discussed, the adaptive scheme could reduce the control effort from the autonomy, thereby making it easier for the human to intervene to avoid the obstacle. Moreover, the human operator also needs to apply more torque in low refresh rate case

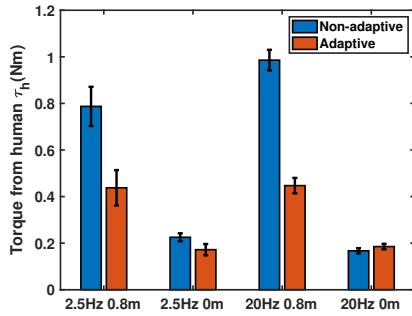


Fig. 8: Control effort in path tracking stage of the driving task for the four conditions of 20 Hz vs. 2.5 Hz refresh rate and 0 m vs. 0.8 m bias in the perception of the path.

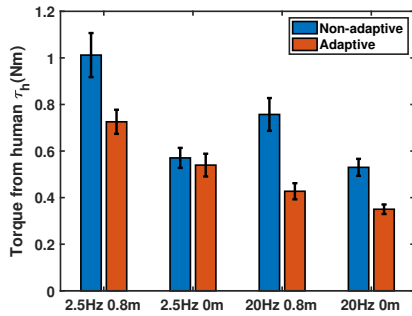


Fig. 9: Control effort in obstacle avoidance stage of the driving task for the four conditions of 20 Hz vs. 2.5 Hz refresh rate and 0 m vs. 0.8 m bias in the perception of the path.

($F(1, 61) = 26.08, p < 0.001$) than the high refresh rate case. The torque in biased case is also significantly higher ($F(1, 61) = 36.9, p < 0.001$) than the non-biased case.

VI. CONCLUSION

This paper presents an adaptive haptic shared control scheme that adjusts the assistance level from the autonomy based on the humans workload. The results indicate that the adaptive haptic shared control scheme can help the human operator use less control effort during the interventions without sacrificing the driving task performance as characterized by the path tracking error.

Some important directions for future work are suggested as a result of limitations in the current study. First, the workload increase due to the bias in autonomy is not accounted for in the design of the assistance level. Taking the effect of bias into account could improve the performance of the adaptive scheme. Second, the adaptive scheme is developed based on a heuristic function as a proof-of-concept. Further research is needed to develop a stronger basis for the function of assistance level.

APPENDIX I

SCALES USED TO MEASURE WORKLOAD AND TRUST

Rate the **Workload** you experienced:



Rate your **Trust** in the shared control autonomy:



REFERENCES

- [1] P. G. Griffiths and R. B. Gillespie, "Sharing control between humans and automation using haptic interface: Primary and secondary task performance benefits," *Human Factors*, vol. 47, no. 3, pp. 574–590, 2005.
- [2] S. M. Petermeijer, D. A. Abbink, and J. C. F. de Winter, "Should drivers be operating within an automation-free bandwidth? Evaluating haptic steering support systems with different levels of authority," *Human Factors*, vol. 57, no. 1, pp. 5–20, 2015.
- [3] A.-T. Nguyen, C. Sentouh, and J.-C. Popieul, "Sensor reduction for driver-automation shared steering control via an adaptive authority allocation strategy," *IEEE/ASME Transactions on Mechatronics*, vol. 23, no. 1, pp. 5–16, 2018.
- [4] A. H. Ghasemi, M. Johns, B. Garber, P. Boehm, P. Jayakumar, W. Ju, and R. B. Gillespie, "Role negotiation in a haptic shared control framework," in *Adjunct Proceedings of the 8th International Conference on Automotive User Interfaces and Interactive Vehicular Applications*, 2016, pp. 179–184.
- [5] M. Mulder, D. A. Abbink, and E. R. Boer, "The effect of haptic guidance on curve negotiation behavior of young, experienced drivers," in *IEEE International Conference on Systems, Man and Cybernetics*, 2008, pp. 804–809.
- [6] W. B. Rouse, S. L. Edwards, and J. M. Hammer, "Modeling the dynamics of mental workload and human performance in complex systems," *IEEE Transactions on Systems, Man and Cybernetics*, vol. 23, no. 6, pp. 1662 – 1671, 1993.
- [7] S. Lu, M. Y. Zhang, T. Ersal, and X. J. Yang, "Workload management in teleoperation of unmanned ground vehicles: Effects of a delay compensation aid on human operators workload and teleoperation performance," *International Journal of Human-Computer Interaction*, vol. 35, no. 19, pp. 1820–1830, 2019.
- [8] D. Kaber and M. Endsley, "The effects of level of automation and adaptive automation on human performance, situation awareness and workload in a dynamic control task," *Theoretical Issues in Ergonomics Science*, vol. 5, no. 2, pp. 113–153, 2004.
- [9] F. Flemisch, F. Nashashibi, N. Rauch, A. Schieben, S. Glaser, G. Temme, P. Resende, B. Vanholme, C. Löper, G. Thomaidis, H. Mosebach, J. Schomerus, S. Hima, and A. Kaußner, "Towards highly automated driving: Intermediate report on the HAVEit-Joint System," in *Proc. 3rd Eur. Road Transp. Res. Arena*, 2010.
- [10] J. Liu, P. Jayakumar, J. L. Stein, and T. Ersal, "Combined speed and steering control in high speed autonomous ground vehicles for obstacle avoidance using model predictive control," *IEEE Transactions on Vehicular Technology*, vol. 66, no. 10, pp. 8746–8763, 2017.
- [11] H. Febbo, J. Liu, P. Jayakumar, J. L. Stein, and T. Ersal, "Moving obstacle avoidance for large, high-speed autonomous ground vehicles," in *American Control Conference*, 2017, pp. 5568–5573.
- [12] J. Liu, P. Jayakumar, J. L. Stein, and T. Ersal, "A nonlinear model predictive control formulation for obstacle avoidance in high-speed autonomous ground vehicles in unstructured environments," *Vehicle System Dynamics*, vol. 56, no. 6, pp. 853–882, 2018.
- [13] H. Febbo, "Nloptcontrol.jl," <https://github.com/JuliaMPC/NLOptControl.jl>, 2017.
- [14] A. Wächter and L. T. Biegler, "On the implementation of an interior-point filter line-search algorithm for large-scale nonlinear programming," *Mathematical Programming*, vol. 106, no. 1, pp. 25–57, 2006.
- [15] Y. Zheng, M. J. Brudnak, P. Jayakumar, J. L. Stein, and T. Ersal, "An experimental evaluation of a model-free predictor framework in teleoperated vehicles," in *IFAC Workshop on Time Delay Systems*, vol. 49, 2016, pp. 157–164.
- [16] S. G. Hart and L. E. Staveland, "Development of NASA-TLX (task load index): Results of empirical and theoretical research," in *Human Mental Workload*, ser. Advances in Psychology, P. A. Hancock and N. Meshkati, Eds. North-Holland, 1988, vol. 52, pp. 139 – 183.
- [17] B. M. Muir and N. Moray, "Trust in automation. Part II. Experimental studies of trust and human intervention in a process control simulation," *Ergonomics*, vol. 39, no. 3, pp. 429–460, 1996.
- [18] X. J. Yang, V. V. Unhelkar, K. Li, and J. A. Shah, "Evaluating effects of user experience and system transparency on trust in automation," in *ACM/IEEE International Conference on Human-Robot Interaction*, 2017, pp. 408–416.
- [19] N. Du, K. Y. Huang, and X. J. Yang, "Not all information is equal: Effects of disclosing different types of likelihood information on trust, compliance and reliance, and task performance in human-automation teaming," *Human Factors*, p. 0018720819862916, 2019. [Online]. Available: <https://doi.org/10.1177/0018720819862916>